Nonlinear dynamics of quantum cascade lasers with optical feedback

L. Jumpertz[a,b*], S. Ferré[b], K. Schires[a], M. Carras[b], and F. Grillot[a]
[a]Telecom Paristech, Ecole Nationale Supérieure des Télécommunications, CNRS LTCI, 46 rue Barrault, 75013 Paris, France ; [b]Alcatel Thales III-V Lab, Campus de Polytechnique, 1 avenue Augustin Fresnel, 91767 Palaiseau, France

ABSTRACT

Quantum Cascade (QC) lasers are widely used in optical communications, high-resolution spectroscopy, imaging, and remote sensing due to their wide spectral range, going from mid-infrared to the terahertz regime. The dynamics of QC-lasers are dominated by their ultrafast carrier lifetime, typically of the order of a few picoseconds. The combination of optical nonlinearities and ultrafast dynamics is an interesting feature of QC-lasers, and investigating the dynamical properties of such lasers gives unprecedented insights into the underlying physics of the components, which is of interest for the next generation of QC devices. A particular feature of QC-lasers is the absence of relaxation oscillations, which is the consequence of the relatively short carrier lifetime compared to photon lifetime. Optical feedback (i.e. self-injection) is known to be a robust technique for stabilizing or synchronizing a free-running laser, however its effect on QC-lasers remains mostly unexplored. This work aims at discussing the dynamical properties of QC-lasers operating under optical feedback by employing a novel set of rate equations taking into account the upper and lower lasing levels, the bottom state as well as the gain stage's cascading. This work analyzes the static laser properties subject to optical feedback and provides a comparison with experiments. Spectral analysis reveals that QC-lasers undergo distinct feedback regimes depending on the phase and amplitude of the reinjected field, and that the coherence-collapse regime only appears in a very narrow range of operation, making such lasers much more stable than their interband counterparts.

Keywords: Quantum cascade laser, optical feedback, nonlinear dynamics.

1. INTRODUCTION

Quantum cascade (QC) lasers were invented in 1994 and are based on intersubband radiative transitions within the conduction band of the material [1]. The device is composed of a succession of active areas and injector zones that electrons cross by tunneling effect. This cascade results in an improved electrical to optical efficiency. The resulting devices are compact semiconductor laser sources emitting either in the mid-infrared (IR) range or in the terahertz (THz) domain, depending on the design of the active area [2]. Much progress has been achieved in the past twenty years and mid-IR QC-lasers emit now typically few hundreds of milliwatts in continuous-wave (CW) operation at room temperature, with thermoelectric cooling. Therefore, QC-lasers have become widely used sources for mid-IR applications such as gas spectroscopy, infrared countermeasures or free-space communications [3].

Nonlinear effects such as those produced by optical feedback have been deeply studied in interband lasers [4-7]. Optical feedback consists in reinjecting part of the laser light after reflection on a mirror or the extremity of an optical fiber. The two main degrees of freedom of optical feedback are the external cavity length L_{ext} and the feedback rate f_{ext}, defined as the ratio between the emitted and the reflected power. By varying these two parameters, five operating regimes can typically be identified [8]. In particular, the laser can either exhibit a fully developed chaotic regime called coherence-collapse and that must strictly be avoided in optical communication systems [9], or operate in a very stable single-mode regime. In the latter, a controlled optical feedback can greatly improve the laser performances in terms of output power, lasing threshold, optical linewidth or modulation bandwidth. This paper aims at studying whether optical feedback has the same impact on QC-lasers as on interband lasers. Regarding the various applications in the mid-IR domain, it is indeed extremely important to understand whether chaos occurs in QC-lasers and how to improve static and dynamical properties of such lasers with a proper external control.

*louise.jumpertz@telecom-paristech.fr

Until now, there have been very few studies dealing with optical feedback in mid-IR QC-lasers. The extended cavity regime, corresponding to very high feedback rates, has been widely used for the realization of external cavity QC-laser [10] taking advantage of a reflection on a Bragg grating to obtain a large tunable source. Moreover, there have been some recent experimental studies on the noise reduction due to optical feedback in QC-lasers [11], and few theoretical studies on the occurrence of chaos in QC-lasers, mainly centered on THz QC-lasers [12,13]. In previous work, we reported for the first time the observation of five feedback regimes in a distributed feedback (DFB) QC-laser emitting at 5.6 µm, similar to those observed with interband lasers [14]. In this work, steady-state results of the QC-laser submitted to optical feedback are derived from a semi-analytical model based on rate equations, and are compared to experiments. A key-parameter controlling the laser dynamics, the so-called linewidth enhancement factor (LEF), is also extracted from the measurements. The paper also discusses the impact of the optical feedback on the spectral stability of both Fabry-Perot (FP) and DFB QC-lasers.

2. NUMERICAL MODEL DESCRIPTION

The numerical description of a QC-laser is complicated to implement. Each active area corresponds to a three-level system in which the electrons tunnel from the injector into level 3, the radiative transition occurring between levels 3 and 2. Then the electron enters level 1 mainly by optical phonon emission, before tunneling into the next injector. Therefore, if N_{pd} is the number of periods, $3\times N_{pd}$ carrier rate equations would have to be solved, leading to a long computation time. In order to allow a semi-analytical treatment of QC laser in presence of optical feedback, a common assumption is to consider a three-level system [15]. In this case, by defining the complex electrical field as $\vec{E} = \sqrt{S}e^{i\varphi}$, we obtain the following set of differential rate equations for the QC-lasers under optical feedback:

$$\frac{dN_3}{dt} = \frac{\eta I}{q} - \frac{N_3}{\tau_{32}} - \frac{N_3}{\tau_{31}} - G_0 \Delta N S \tag{1}$$

$$\frac{dN_2}{dt} = \frac{N_3}{\tau_{32}} - \frac{N_2}{\tau_{21}} + G_0 \Delta N S \tag{2}$$

$$\frac{dN_1}{dt} = \frac{N_3}{\tau_{31}} + \frac{N_2}{\tau_{21}} - \frac{N_1}{\tau_{out}} \tag{3}$$

$$\frac{dS}{dt} = \left(N_{pd} G_0 \Delta N - \frac{1}{\tau_p}\right) S + \beta \frac{N_3}{\tau_{sp}} + 2k\sqrt{S(t-\tau_{ext})S(t)}\cos(\Delta\varphi) \tag{4}$$

$$\frac{d\varphi}{dt} = \frac{\alpha}{2}\left(N_{pd} G_0 \Delta N - \frac{1}{\tau_p}\right) - k\sqrt{\frac{S(t-\tau_{ext})}{S(t)}}\sin(\Delta\varphi) \tag{5}$$

In equations (1) to (5), N_j is the carrier density of level j, with $\Delta N = N_3 - N_2$, η the conversion efficiency, I the bias current while τ_{ij} corresponds to the carrier lifetime from level i to level j, τ_{out} the characteristic time for the electron to tunnel into the injector, τ_{sp} the spontaneous emission lifetime, and τ_p the photon lifetime inside the laser cavity. Finally G_0 represents the net modal gain, α the LEF and β the spontaneous emission coefficient. $\Delta\varphi$ is defined as $\Delta\varphi = \omega_0\tau_{ext} + \varphi(t) - \varphi(t-\tau_{ext})$, with τ_{ext} the external cavity roundtrip time. Finally, k is the feedback coefficient, defined as:

$$k = \frac{1}{\tau_{in}} \frac{1-R_2}{\sqrt{R_2}} \sqrt{f_{ext}} \tag{6}$$

where τ_{in} is the internal cavity roundtrip time and R_2 the reflectivity of the laser facet directed toward the external cavity. In equation (4), let us stress that the spontaneous emission term will be neglected since its characteristic time is three orders of magnitude slower than other lifetimes.

The steady-state solutions to these rate equations are given by $dN_i/dt=0$ and $dS/dt=0$ and can be expressed as follows:

$$N_3 = \frac{\tau_{31}\tau_{21}}{\tau_{31}+\tau_{21}}\left[\frac{\eta I}{q} + \frac{1}{N_{pd} G_0 \tau_{21}}\left(\frac{1}{\tau_p} - 2k\cos(\omega_s \tau_{ext})\right)\right] \tag{7}$$

$$N_2 = \frac{\tau_{31}\tau_{21}}{\tau_{31}+\tau_{21}}\left[\frac{\eta I}{q} - \frac{1}{N_{pd}G_0\tau_{31}}\left(\frac{1}{\tau_p} - 2k\cos(\omega_s\tau_{ext})\right)\right] \quad (8)$$

$$\Delta N = \frac{1}{N_{pd}G_0}\left(\frac{1}{\tau_p} - 2k\cos(\omega_s\tau_{ext})\right) \quad (9)$$

$$N_1 = \tau_{out}\frac{\eta I}{q} \quad (10)$$

$$S = \frac{N_{pd}}{1/\tau_p - 2k\cos(\omega_s\tau)}\frac{1}{\tau_{32}(\tau_{31}+\tau_{21})}\left[\tau_{31}(\tau_{32}-\tau_{21})\frac{\eta I}{q} - \frac{\tau_{32}+\tau_{31}}{N_{pd}G_0}\left(\frac{1}{\tau_p} - 2k\cos(\omega_s\tau_{ext})\right)\right] \quad (11)$$

$$\varphi(t) = (\omega_s - \omega_0)t \quad (12)$$

From equation (5), we can furthermore deduce:

$$\omega_s - \omega_0 = -k[\alpha\cos(\omega_s\tau_{ext}) + \sin(\omega_s\tau_{ext})] \quad (13)$$

Steady state configurations in particular those from Eq. (5) correspond to the external cavity modes that drive the dynamical properties of QC-laser through the occurrence of both stable and instable solutions.

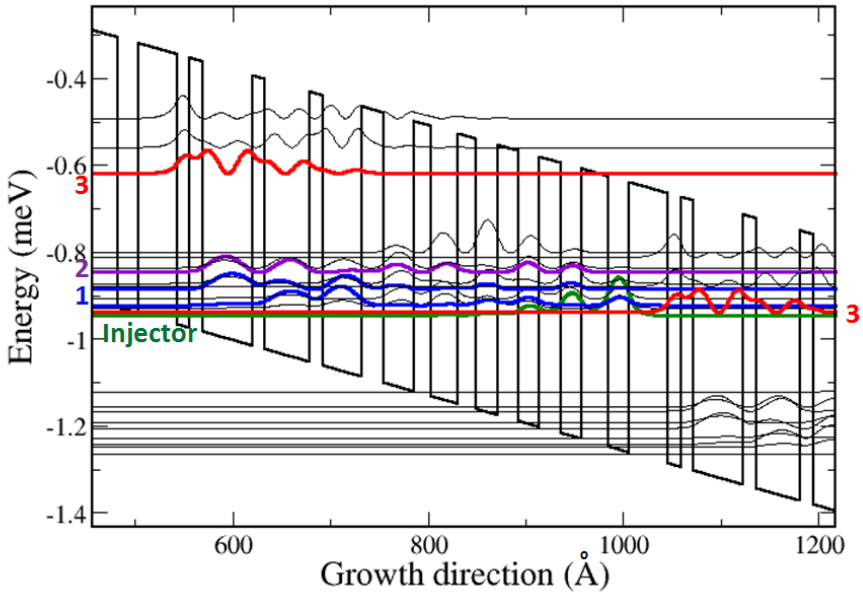

Figure 1. Three level system in a QC-laser. The radiative transition occurs between levels 3 and 2. Level 1 is split due to the two phonons absorption model. After passing through the injector, the carrier reaches level 3 of the next period.

3. EXPERIMENT DESCRIPTION

The lasers used for the experiment are FP or DFB QC-lasers emitting around 5.6 µm. These structures have the same AlInAs/GaInAs active area based on the design proposed in [16]. The active region was grown by molecular beam epitaxy (MBE) on InP, then the upper cladding in InP was grown by metal organic chemical vapor epitaxy (MOCVE). For DFB lasers, single-mode operation is guaranteed by a top metal grating [17] with a coupling efficiency $\kappa = 4\ cm^{-1}$. The active area dimensions are 9 µm over 2 mm for the DFB lasers and 6 µm over 4 mm for the FP QC-lasers. Both lasers have a high-reflectivity coating on the back facet to increase their conversion efficiency.

Simulation electronic parameters were calculated within the framework of a broad purpose custom heterostructure simulation software, METIS [18]. Based on semi-classical Boltzmann-like equation with thermalized subbands [19], optical and acoustic longitudinal phonons, roughness scattering, coherent tunneling through the barrier, absorption of photons, stimulated and spontaneous emission were taken into account. Within this formalism we obtained the potential,

energy states, wave functions (shown in Figure 1) as well as electronic scattering times. These parameters and other useful ones are summarized in Table 1.

Table 1. Parameters of the lasers under study

Parameter	Value	Parameter	Value
Conversion efficiency η	0.12	Number of periods N_{pd}	30
Carrier lifetime 3→2 τ_{32}	2.27 ps	Group index n_g	3.2
Carrier lifetime 3→1 τ_{31}	2.30 ps	Facet reflectivity R_2	0.3
Carrier lifetime 2→1 τ_{21}	0.37 ps	Net modal gain G_0	1.2×10^4 s^{-1}
Carrier escape time τ_{out}	0.54 ps	Photon lifetime τ_p	4.74 ps

The QC-laser described in the previous section is inserted in the experimental setup presented in Figure 2. The laser light is collimated and split into a reinjection path and a detection path using a 60/40 beam splitter. The reflection part consists of a mirror and a polarizer tuning the feedback rate to up to 37%. This important parameter is furthermore controlled in real-time by using a power-meter. Using this setup, the external cavity length can be tuned between 13 and 95 cm corresponding to an external roundtrip time between 1 ns and 6 ns. The detection path is sent either to a power-meter for L-I characteristic curves measurement, or to a Fourier transform IR (FTIR) spectrometer, allowing measurement of optical spectra with a resolution of 0.125 cm^{-1}.

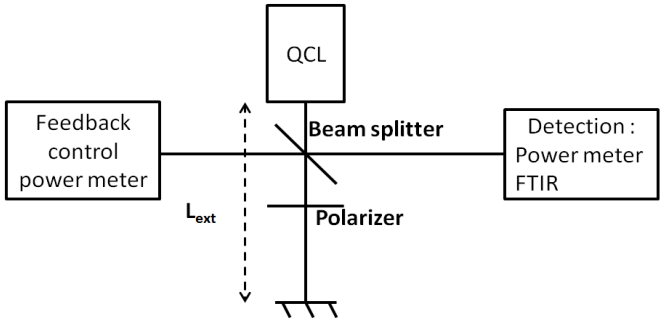

Figure 2. Experimental set-up

4. EXTRACTION OF THE LINEWIDTH ENHANCEMENT FACTOR

The LEF or α-factor, introduced for the first time by Henry in 1982, plays a crucial role in semiconductor devices and systems. It describes the coupling between the carrier-induced variations of the real and imaginary parts of the optical susceptibility. In semiconductor lasers, the LEF affects many static and dynamical aspects, such as spectral broadening, mode stability, frequency chirp under current modulation, and nonlinear dynamics subject to an external control such as optical injection or feedback. It is also responsible for the filamentation in broad-area lasers [20].

In most cases, the measurement of the LEF is based on the sub-threshold method originally proposed by Hakki and Paoli, which consists in extracting both the net modal gain and the modal wavelength from the amplified spontaneous emission (ASE) spectrum [21]. This method is thus only applicable below threshold and does not correspond to an actual lasing condition. More reliable techniques to measure the above-threshold LEF have been developed and are based on optical injection, self-mixing, or direct modulation. From equation (13), we can furthermore deduce a simple expression to obtain the LEF of the QC-laser from our optical feedback experiment that can be written as

$$\alpha = \frac{\omega_0 - \omega_s}{k\cos(\omega_s \tau_{ext})} - \tan(\omega_s \tau_{ext}) \quad (14)$$

An equivalent expression has already been used to determine the LEF in interband lasers, and has given consistent results. Since the model is only valid for a single-mode laser, the LEF measurements have been firstly realized on a FP laser by following with the FTIR the wavelength shift of one lasing mode with the feedback rate (Figure 3). Further work will involve the LEF extraction of the DFB laser. However for DFB lasers the expression of k is no longer valid and needs to be properly derived for a QC-structure, in a more complex way than for interband DFB optical sources [22].

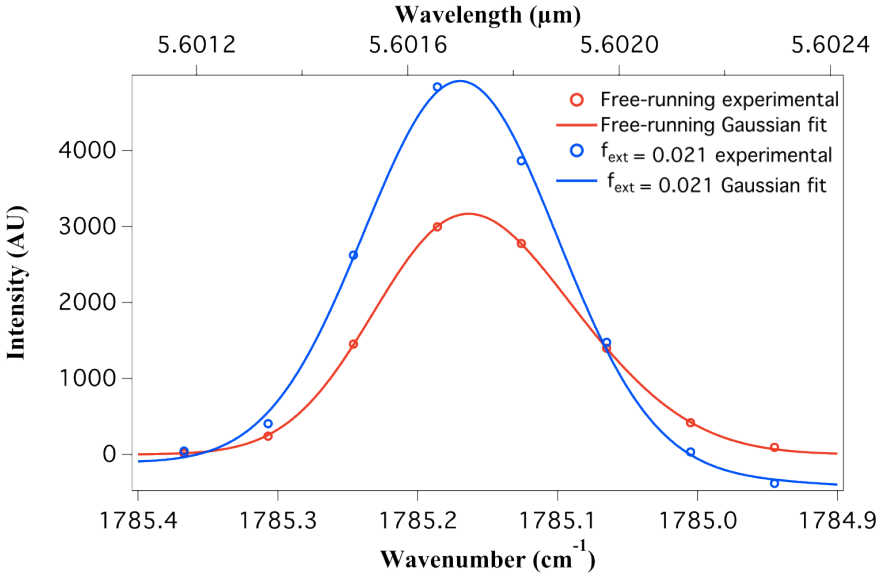

Figure 3. Gaussian fits (lines) and experimental data (dots) of one laser mode for the free-running case and for f_{ext}=0.021, showing the lasing wavelength evolution with optical feedback.

With this method, the LEF of the FP laser is estimated to be about $\alpha = 1.3 \pm 0.5$. This value is consistent with the typical LEF found in the literature for mid-IR QC-lasers. Although the magnitude of the optical feedback is relatively strong in the experiments under study, it is important to point out that the LEF does not evolve significantly with feedback, as already observed in interband lasers.

5. L-I CHARACTERISTIC CURVES

Figure 4a presents the experimental light vs. current characteristic curves (L-I curves) of the FP QC-laser for several feedback ratios with an external cavity length of 13 cm. Measurements show that optical feedback induces a significant threshold current reduction of up to 6.5% of its free-running value, as well as an increase of output power. It is however worth noting that the maximum optical power is not obtained for the highest feedback rate.

The analysis of the L-I curves also points out the apparition of undulations for high feedback rates. This phenomenon that also appears in interband lasers is due to interferences between the internal and external cavity modes [23]. The heating of the active area when increasing the bias current will indeed modify the refractive index, and therefore the effective internal cavity length of the laser, causing the interferences to be alternatively constructive or destructive, hence the power fluctuations. Since this effect is linked to the temperature evolution of the active area, the L-I curves present a strong hysteresis, as shown in Figure 4 b).

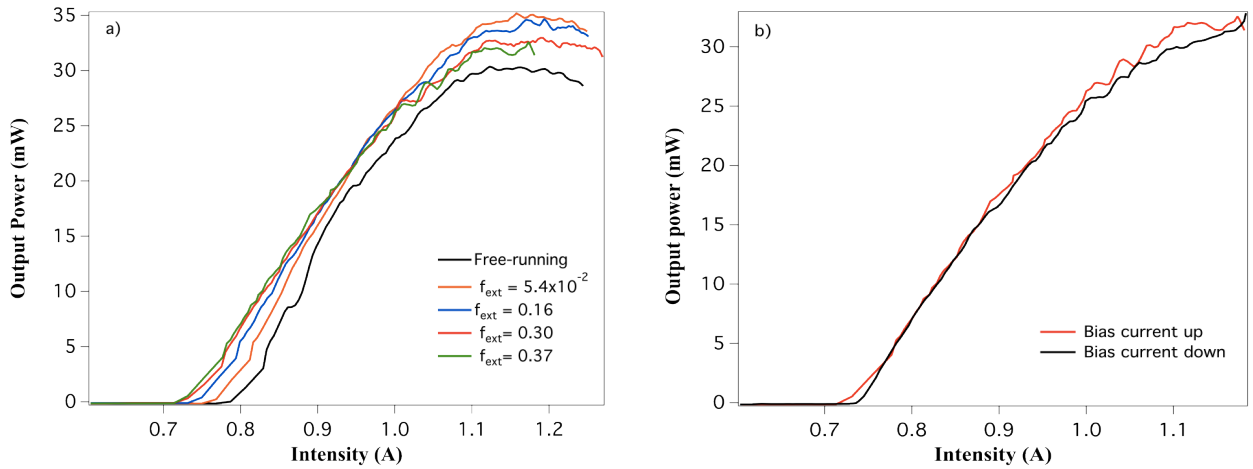

Figure 4. a) L-I characteristic curves for several feedback rates. b) Apparition of hysteresis for high feedback values ($f_{ext} = 0.37$).

Equation (11) allows retrieving the threshold current as a function of the feedback parameters.

$$I_{th} = \frac{q}{\eta}\frac{\tau_{32}+\tau_{31}}{\tau_{31}(\tau_{32}-\tau_{21})}\frac{1}{N_{pd}G_0}\left(\frac{1}{\tau_p} - 2kcos(\omega_s\tau_{ext})\right) \quad (15)$$

The lasing frequency under feedback ω_s is selected among the solutions of eq. 13 as the one for which ΔN reaches a minimum. Experimental and numerical results are in excellent agreement, as presented in Figure 5.

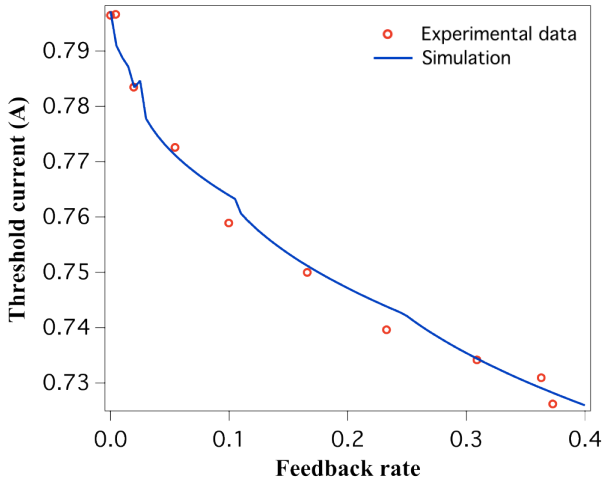

Figure 5. Threshold reduction with optical feedback, experimental data (dots) and numerical simulation (dashed line).

6. IDENTIFICATION OF THE FEEDBACK REGIMES

As already discussed in [14], by analyzing the optical spectra shown in Figure 6 a) we were able to identify for the first time five feedback regimes for the DFB QC-laser, very similar to the ones observed in interband lasers. The first regime, for very low feedback rates, corresponds to a stable single-mode operation at the DFB wavelength. Furthermore the amplitude of the lasing mode is phase-dependent, although the limited FTIR resolution did not allow us to conclude whether the linewidth is also phase-dependent as in the case of interband lasers. The second regime exhibits a beating between two adjacent modes of the FP cavity that is also phase-dependent. In the third regime the laser re-stabilizes in a single external cavity mode, hence not lasing at the DFB mode, and corresponding in interband lasers to the lowest

linewidth mode. Further measurements are required to confirm whether this is the case in QC-lasers as well. As the feedback level is further increased, the laser undergoes a transition to a fourth regime that appears to be unstable, with an increase of the spectrum pedestal and a diminution of the side-mode suppression ratio. Finally, the fifth regime is stable and corresponds to a single-mode emission at the DFB frequency with high output power. This corresponds to the extended cavity regime, where the laser is equivalent to a small active area in a long cavity, one of the cavity mirrors being the feedback mirror. This is also the regime used in external-cavity QC-lasers.

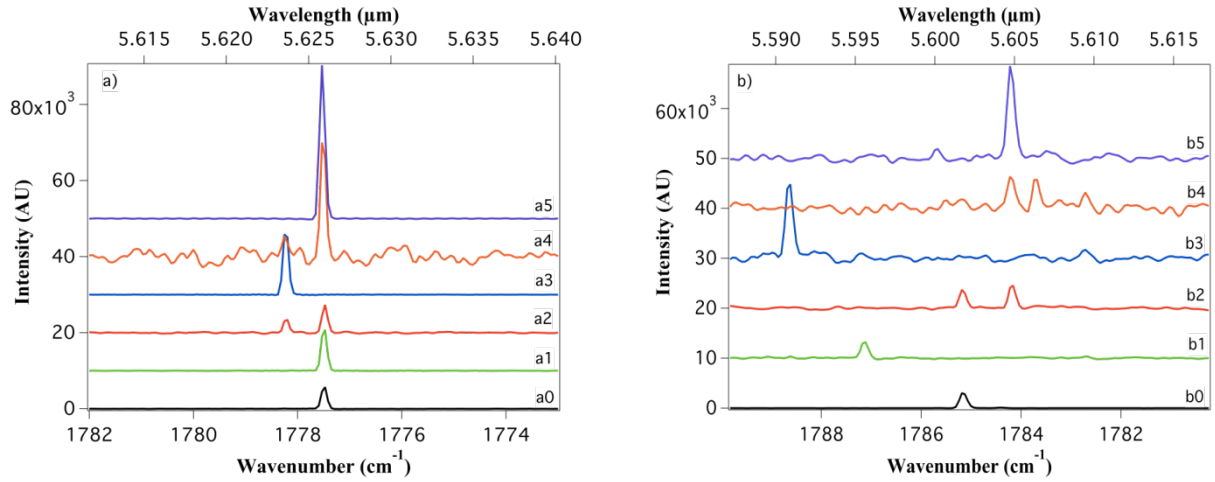

Figure 6. FTIR spectra with several feedback rates and an external cavity length of 15 cm. a) DFB QC-laser. a0: Free-running case. a1: Regime 1, $f_{ext} = 9.1 \times 10^{-4}$. a2: Regime 2, $f_{ext} = 5.1 \times 10^{-3}$. a3: Regime 3, $f_{ext} = 3.2 \times 10^{-2}$. a4: Regime 4, $f_{ext} = 0.13$. a5: Regime 5, $f_{ext} = 0.25$. b) FP QC-laser. b0: Free-running case. b1: Regime 1, $f_{ext} = 1.4 \times 10^{-3}$. b2: Regime 2, $f_{ext} = 1.7 \times 10^{-2}$. b3: Regime 3, $f_{ext} = 0.14$. b4: Regime 4, $f_{ext} = 0.18$. b5: Regime 5, $f_{ext} = 0.25$.

In the feedback cartography of interband lasers, the fourth regime is called the coherence-collapse regime and corresponds to the apparition of optical chaos. Coherence collapse is the common name given to describe the irregular dynamics occurring when the laser is operated above threshold. This regime has been described as co-existing chaotic attractors and as an important source of instabilities. The main consequence of the coherence collapse regime consists in a drastic collapse of the laser's coherence time leading to a strong spectral broadening, an increase of the electrical spectrum pedestal, the apparition of periodic and chaotic oscillations on the time-series and the diminution of the side-modes extinction ratio on the optical spectra. With the FTIR resolution, we were not able to observe a clear linewidth increase, therefore further study and especially the analysis of electrical spectra and time-series is on-going to determine whether the fourth regime does indeed correspond to chaos in QC-lasers. As presented in Figure 6 b), similar feedback regimes were observed in the FP QC-laser although the side-mode extinction ratio is not as high as for DFB QC-lasers in the stable regimes. We can see that the wavelength varies strongly with optical feedback, as it is not determined by the DFB grating.

7. CONCLUSION

In this work, we have presented experimental results on FP and DFB QC-lasers submitted to optical feedback. Five feedback regimes close to the ones observed in interband lasers have been identified, although further study is necessary to determine whether the fourth regime indeed corresponds to chaos. Optical feedback has furthermore an impact on the output power and threshold current of the laser and these results are coherent with the steady-state numerical analysis. Therefore, optical feedback appears to be an efficient method to significantly improve the static properties of QC-lasers for applications such as gas spectroscopy or free-space communications.

ACKNOWLEDGMENTS

This work is supported by the French Military Agency (DGA).

REFERENCES

[1] Faist J., Capasso F., Sivco D. L., Sirtori C., Hutchinson A. L. and ChoA. Y.,"Quantum Cascade Laser", Science, 264(5158), 553–556 (1994).
[2] Gmachl C., Capasso F., Sivco D. L. and Cho A. Y., "Recent progress in quantum cascade lasers and applications.", Reports on Progress in Physics, 64(11), 1533 (2001).
[3] Capasso F., Paiella R., Martini R., Colombelli R., Gmachl C., Myers T. L., Taubman M. S., Williams R. M., Bethea C. G., Unterrainer K., Hwang H. Y., Sivco D. L., Cho A. Y., Sergent A. M., Liu H. C. and Whittaker E. A., "Quantum cascade lasers: ultrahigh-speed operation, optical wireless communication, narrow linewidth, and far-infrared emission." IEEE Journal of Quantum Electronics, 38(6), 511–532 (2002).
[4] Favre F., Le Guen D. and Simon J.-C., "Optical Feedback Effects Upon Laser Diode Oscillation Field Spectrum." IEEE Transactions on Microwave Theory and Techniques, 30(10), 1700–1705 (1982).
[5] Goldberg L., Taylor H. F., Dandridge A., Weller J. F. and MilesR., "Spectral characteristics of semiconductor lasers with optical feedback." IEEE Journal of Quantum Electronics, 18(4), 555–564 (1982).
[6] Osmundsen J. and Gade N., "Influence of optical feedback on laser frequency spectrum and threshold conditions." IEEE Journal of Quantum Electronics, 19(3), 465–469 (1983).
[7] Peterman K., "External optical feedback phenomena in semiconductor lasers." IEEE Journal of Selected Topics in Quantum Electronics, 1(2), 480–489 (1995).
[8] Tkach R. W. and Chraplyvy A. R., "Regimes of feedback effects in 1.5μm distributed feedback lasers." Journal of Lightwave Technology, 4(11), 1655–1661 (1986).
[9] Lenstra D., Verbeek B. and Den Boef A., "Coherence collapse in single-mode semiconductor lasers due to optical feedback." IEEE Journal of Quantum Electronics, 21(6), 674–679 (1985).
[10] Hugi A., Maulini R. and Faist J., "External cavity quantum cascade laser." Semiconductor Science and Technology, 25(8), 083001 (2010).
[11] Weidmann D., Smith K., and Ellison B., "Experimental investigation of high-frequency noise and optical feedback effects using a 9.7 μm continuous-wave distributed-feedback quantum-cascade laser." Appl. Opt., 46(6), 947–953 (2007).
[12] Mezzapesa F. P., Columbo L. L., Brambilla M., Dabbicco M., Borri S., Vitiello M. S., Beere H. E., Ritchie D. A. and Scamarcio G., "Intrinsic stability of quantum cascade lasers against optical feedback." Opt. Express, 21(11), 13748–13757 (2013).
[13] Columbo L. L. and Brambilla M., "Multimode regimes in quantum cascade lasers with optical feedback." Opt. Express, 22(9), 10105–10118 (2014).
[14] Jumpertz L., Carras M., Schires K. and Grillot F., "Regimes of external optical feedback in 5.6 μm distributed feedback mid-infrared quantum cascade lasers." Applied Physics Letters, 105(13) (2014).
[15] Rana F. and Ram R. J., "Current noise and photon noise in quantum cascade lasers". Phys. Rev. B, 65, 125313 (2002).
[16] Evans A., Yu J. S., David J., Doris L., Mi K., Slivken S. and Razeghi M., "High-temperature, high-power, continuous-wave operation of buried heterostructure quantum-cascade lasers." Applied Physics Letters, 84(3), 314–316 (2004).
[17] Carras M., Maisons G., Simozrag B., Garcia M., Parillaud O., Massies J. and Marcadet X., "Room-temperature continuous-wave metal grating distributed feedback quantum cascade lasers." Applied Physics Letters, 96(16), 161105 (2010).
[18] Trinité, V., Ouerghemmi, E., Guériaux, V., Carras, M., Nedelcu, A., Costard, E., & Nagle, J., "Modelling of electronic transport in quantum well infrared photodetectors", Infrared Physics & Technology, 54(3), 204-208 (2011).
[19] Mc Tavish, J., Indjin, D., & Harrison, P., "Aspects of the internal physics of InGaAs⁄ InAlAs quantum cascade lasers", Journal of Applied Physics, 99(11), 114505 (2006).
[20] Provost J. and Grillot F., "Measuring the chirp and the linewidth enhancement factor of optoelectronic devices with a Mach-Zehnder interferometer". IEEE Photonics Journal, 3(3), 476–488 (2011).
[21] Hakki B. W. and Paoli T. L., "Gain spectra in Ga/As double heterostructure injection lasers." Journal of Applied Physics, 46(3), 1299–1306 (1975).
[22] Grillot F., "On the effects of an antireflection coating impairment on the sensitivity to optical feedback of Ar/Hr semiconductor DFB lasers." IEEE Journal of Quantum Electronics, 45(6), 720–729 (2009).
[23] Lang R. and Kobayashi K., "External optical feedback effects on semiconductor injection laser properties." IEEE Journal of Quantum Electronics, 16(3), 347–355 (1980).